



HAL
open science

Comparison of interface models to account for surface tension in SPH method

Sandra Geara, S. Adami, Sylvain Martin, Olivier Bonnefoy, J. Allenou, B. Stepnik, W. Petry

► To cite this version:

Sandra Geara, S. Adami, Sylvain Martin, Olivier Bonnefoy, J. Allenou, et al.. Comparison of interface models to account for surface tension in SPH method. PARTICLES 2019 - VI International Conference on Particle-Based Methods. Fundamentals and Applications, International Center for Numerical Methods in Engineering (CIMNE); Universitat Politècnica de Catalunya (UPC); European Community on Computational Methods in Applied Sciences (ECCOMAS); International Association for Computational Mechanics (IACM), Oct 2019, Barcelona, Spain. pp.714 à 725. emse-02442782

HAL Id: emse-02442782

<https://hal-emse.ccsd.cnrs.fr/emse-02442782v1>

Submitted on 16 Jan 2020

HAL is a multi-disciplinary open access archive for the deposit and dissemination of scientific research documents, whether they are published or not. The documents may come from teaching and research institutions in France or abroad, or from public or private research centers.

L'archive ouverte pluridisciplinaire **HAL**, est destinée au dépôt et à la diffusion de documents scientifiques de niveau recherche, publiés ou non, émanant des établissements d'enseignement et de recherche français ou étrangers, des laboratoires publics ou privés.

Comparison of interface models to account for surface tension in SPH method

S. Geara*^{a,c,d}, S. Adami^b, S. Martin^a, O. Bonnefoy^a, J. Allenou^c, B. Stepanik^c, W. Petry^d

^aMines Saint-Etienne, Univ Lyon, CNRS, UMR 5307 LGF
Centre SPIN, F - 42023 Saint-Etienne, France

^bChair of Aerodynamics and Fluid Mechanics,
Technical University of Munich, Garching, Germany

^cFramatome - CERCATM
10 Rue Juliette Récamier, 69456 Lyon Cedex 06, France

^dResearch Neutron Source Heinz Maier-Leibnitz (FRM II),
Technical University of Munich, 85748 Garching, Germany

ABSTRACT

The Smoothed Particle Hydrodynamics method (SPH) is a meshfree Lagrangian simulation method widely applied for fluid simulations due to the advantages presented by this method for solving problems with free and deformable surfaces.

In many scientific and engineering applications, surface tension forces play an important or even dominating role in the dynamics of the system. For instance, the breakage (instability) of a liquid jet or film is strongly affected by the strength of the surface tension at the liquid-air interface. Simulating deforming phase interfaces with strong topological changes is still today a challenging task. As a promising numerical method, here we use SPH to predict the interface instability at a water-air interface.

With SPH, the main challenge in modelling surface tension at a free-surface is the accurate description of the interface (normal direction and curvature). When only the liquid phase is modelled (to decrease the computational cost), the standard SPH approximations to calculate the normal direction and curvature of the interface suffer from a lacking “full support”, i.e. the omitted and therefore missing gas particles. Various models for such free surface surface tension corrections were presented, see e.g. among others Sirotkin et al., Ordoubadi et al. or Ehigiamusoe et al. Many of these models follow the classical Continuum Surface Force (CSF) approach (Morris, Adami et al.) and incorporate different corrections/treatments at the surface.

The objective of our ongoing study is to investigate the influence of different interface descriptions. We compare different free surface particle detection schemes, normal vector calculations and curvature estimations for the quality of the resulting surface-tension effect. In this work, we focus on two-dimensional problems and consider a static drop and oscillating drops as test cases.

KEYWORDS

Smoothed Particle Hydrodynamics, Free surface flow, Surface tension, Interface description

I. Introduction

Surface tension plays an important role in many engineering and industrial applications such as liquid atomization. Usually, these phenomena occur on small length scales, therefore the development of a proper surface tension model can help greatly in physically developing these applications. However, simulating deforming phase interfaces with strong topological changes is still today a challenging task.

Among existing methods for fluid simulations, the Smoothed Particle Hydrodynamics (SPH) presents the advantage of simulating free surfaces with high deformations. SPH is a meshfree Lagrangian numerical method that was first introduced independently in 1977 by Lucy [1] and Gingold and Monaghan [2] to solve astrophysical problems. The general idea behind SPH lies in representing the fluid by a series of discretization points/particles each representing a mass of fluid. The continuity of the fluid and its properties is recovered by the spatial convolution of the physical properties of each particle by a kernel or smoothing function.

Three general approaches for modeling surface tension with SPH can be found in the literature. The first one is the Inter Particle Force (IPF) where an attractive/repulsive force is applied to all the SPH particles [3], [4]. The implementation of the IPF is simple. However, the main drawback of this method is that the surface tension force needs to be calibrated with experimental results. The second one is the Continuum Surface Stress (CSS), where the surface tension force is formulated as a gradient of the stress tensor which is calculated from the surface normal with no need to calculate the curvature [5]. The third one is the Continuum Surface Force (CSF), initially proposed by Brackbill [6], where the surface tension force is converted to a force per unit volume and is applied only on particles close to the interface. The main challenge of this method is to accurately calculate the normal vectors and the curvature at the interface. In this work we are focusing on the CSF method because it is a general approach that uses the physical properties of the fluid and does not need to be tuned for each simulation case. Many of the CSF models found in the literature are only valid for fluid-fluid systems [7], [8]. However, for free surfaces, the standard SPH approximations to calculate the normal vector and curvature of the interface suffer from the lack of “full support”, i.e. the omitted and therefore missing gas particles. To overcome this problem many corrections were proposed in the literature, see e.g. amongst others [9]–[12].

In their model, Sirotkin *et al.* [9] used the correction matrix proposed by Bonet *et al.* [13] to adjust the kernel gradient for the calculation of the density, pressure force, normal vectors and curvature. This kernel gradient modification allows to obtain accurate normal vectors and curvature estimations, however a 1.5 times bigger smoothing length is required for more reliable results. Ordoubadi *et al.* [10] added imaginary particles near the free surface with a mirroring technique in order to accurately simulate the surface tension force. This technique seems complex to implement and not straightforward, but according to the examples shown it significantly improves the normal vectors and gives more accurate curvatures. However, in all their examples a high fluid viscosity was used (100 times the viscosity of water). Ehigiamusoe *et al.* [11] used a correction factor for only the curvature calculation without any additional correction for the normal vectors. This method may give stable and accurate results for simple examples, but in the cases with sharp corners and high surface deformation, another correction technique needs to be used for the normal vector calculation and curvature estimation. Russel *et al.* [12] adapted the model proposed by Morris [7] for free surface simulations by proposing a correction factor for the normal vectors and curvatures. However, once again this correction factor is valid only for simple cases but not for complex geometries with sharp edges or sudden changes in the curvature. It is worth mentioning that in most of the presented models the numerical validation examples were conducted at relatively high fluid viscosities.

The objective of our ongoing study is to investigate the influence of the interface properties estimation in the presented models on the surface tension force. We compare different free surface particle detection schemes, normal vector calculations and curvature estimations for the quality of the resulting surface-tension effect. In this work, we focus on two-dimensional problems and consider a static drop with Laplace law and oscillating drops as representative test cases.

II. Basics of SPH method

In the Lagrangian description, the Navier-Stokes set of equations for viscous flow can be expressed as

$$\frac{d\rho}{dt} = -\rho \nabla \cdot v \quad (1)$$

$$\frac{dv}{dt} = g + \frac{1}{\rho} [-\nabla P + F^{(v)} + F^{(s)}] \quad (2)$$

where ρ , v , g , P , $F^{(v)}$, $F^{(s)}$ are density, velocity, body force, pressure, viscous force and surface tension force, respectively.

The idea of SPH is the discretization of the domain with a set of particles and the use of weighted integrals to approximate the field functions. The value of any function f (e.g. density or velocity) at a position r can be estimated according to the following summation form

$$f(\vec{r}) \approx \sum_j^N \frac{m_j}{\rho_j} f(\vec{r}_j) W(|\vec{r}_i - \vec{r}_j|, h), \quad (3)$$

where m_j and r_j are the mass and position of particle j , respectively. W represents the weighting kernel function with h being the smoothing length that determines the interpolation domain. A suitable kernel function should be normalized, positive and radially symmetric. It should converge to the Dirac delta function when h tends to 0 and it should have a compact support domain [14]. Here we use the Spike 3 kernel function (with a compact support of $3h$) because it minimizes the instability due to compression [9].

Using Eq. (3), various SPH formulations can be obtained depending on the assumptions and purpose of the simulation [15]. In our study, we used the formulation proposed by Adami [8].

According to the CSF approach, the surface tension force is applied in the normal direction only on particles near the free surface to minimize the surface energy. It can be expressed as follows [7]

$$f^{(s)} = \delta_s \sigma k \hat{n} \quad (4)$$

where δ_s is the surface delta function used to smooth the surface tension force over a transition band, σ is the surface tension coefficient, k the curvature and \hat{n} the normalized normal vector.

The accurate representation of the surface tension force at the interface depends on the normal vector calculation and curvature estimation.

III. Surface topology characterization

III.1. Surface particle detection

For multi-phase simulations a color function assigned to each particle is used to track the interface. The smoothing of the color function is defined as

$$c_i = \sum_j c_j^0 V_j W_{ij}, \quad (5)$$

where c_j^0 is the color function. For single-phase simulations the color function of all fluid particles is equal to 1.

For Eq. (5) the value of c_i is theoretically equal to 1 for particles in the bulk with a full kernel support, while close to the free surface the number decreases. A threshold value of 0.9 can be defined for detecting surface particles. This method (Kernel summation) is very simple to implement and does not have a large computational cost. It presents the advantage of detecting a surface band instead of only surface particles by adjusting the threshold value. However, in some simulations, low density regions may appear inside the fluid. In these regions, spurious free surface particles can be detected due to the lack of neighboring particles, inducing non physical surface tension forces.

To avoid this problem, more accurate surface tracking algorithms were developed. Barecasco *et al.* [16] presented a simple method for detecting free-surface particles based on the idea of cover vectors. For each particle i , the cover vector b_i is defined as

$$b_i = \sum_j \frac{\vec{r}_i - \vec{r}_j}{|\vec{r}_i - \vec{r}_j|} \quad (6)$$

For detecting surface particles, a cone of angle θ_i (threshold angle) is considered around each b_i . If one of the neighboring particles j is inside the cone, then particle i is not considered as a surface particle, otherwise particle i belongs to the free surface. The value of θ_i plays an important role in boundary particle detection, it is usually chosen equal to $\pi/3$.

Another accurate surface particle detection algorithm [17] is to consider a disk, having twice the length of the supporting domain for good accuracy, around each particle i . This circular area is then split into sectors (in our case 8 sectors are considered), and each sector is checked for neighboring fluid particles. If at least one sector does not have any particle, than particle i is considered as surface particle.

Figure 1 shows a comparison between the three described methods for a classical dam break simulation. Surface particles can be detected by these methods even when the surface undergoes major deformations. As explained earlier, with the first method, cavities inside the fluid can be wrongly detected as free-surface, see Figure 1 a) (right side).

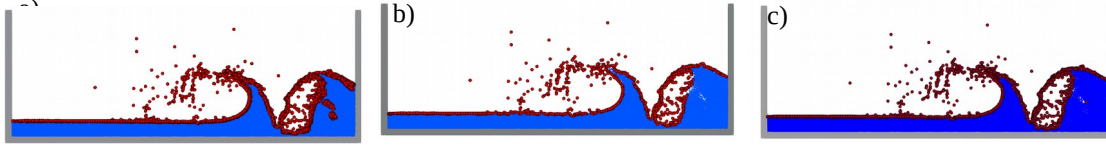


Figure 1: Surface particle detection (red particles represent surface particles): a) Kernel summation, b) Cover vector and c) Disk sectors

Because the two last methods are more time-consuming compared to the simple summation (Figure 2), it is interesting to combine these two techniques [10]. The first step consists of detecting the surface particles by the Kernel summation technique and then "Cover vector" (b) or "Disk sectors" (c) can be performed only on these surface particles.

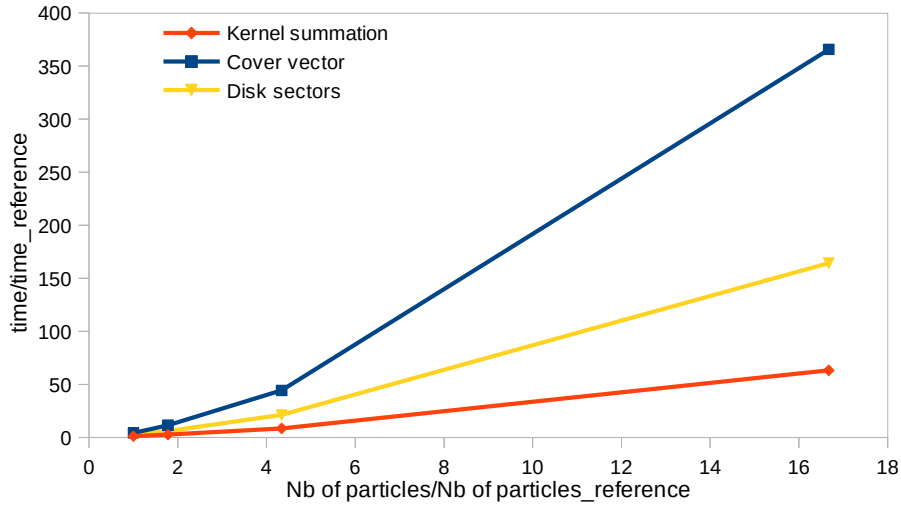


Figure 2: Computational time as a function of the number of particles

III.2. Normal vectors

Many of the CSF surface tension models are based on the model presented by Morris [7]. The normal vectors can be estimated as the gradient of the color function

$$\vec{n}_i = \vec{\nabla} c_i \quad (7)$$

$$\text{with } \vec{\nabla} c_i = \sum_j V_j (c_j - c_i) \vec{\nabla} W_{ij} \quad \text{"NV-Color gradient"} \quad (8)$$

where c_i is calculated according to Eq. (3).

When modeling only one phase, the number of interpolation points decreases near the free surface. One of the techniques that can be used to overcome this problem is the correction matrix proposed by Bonet *et al.* [13] to adjust the kernel gradient. Sirotkin *et al.* [9] used this correction matrix for the density, pressure force, normal vector and curvature calculation. For each particle i the matrix L_i is defined as

$$L_i = \sum_j V_j (\vec{\nabla} W_{ij}) \otimes \vec{r}_{ij} \quad (9)$$

$$\vec{\nabla} \widetilde{W}_{ij} = L_i^{-1} \vec{\nabla} W_{ij} \quad (10)$$

With this new correction for the kernel gradient, the normal vector for each particle i becomes

$$\vec{\nabla} c_i = \sum_j V_j (c_j - c_i) \vec{\nabla} \widetilde{W}_{ij} \quad \text{"NV-Color gradient corrected"} \quad (11)$$

Based on Eq. (7), Russel *et al.* [12] proposed the following normal vector calculation

$$\vec{n}_i = \sum_j V_j \left(\frac{1}{c_i} + \frac{1}{c_j} \right) \vec{\nabla} W_{ij} \quad \text{"NV-Russel *et al.*"} \quad (12)$$

Ordoubadi *et al.* [10] proposed another method that consists of adding imaginary particles by mirroring the particles in the transition band. These particles have the same mass as particle i with a color function equal to zero. If particle i is a surface particle, then for each particle j located in the support domain of i (but not a surface particle), a particle j' is created by mirroring particle j according to i. Otherwise, if particle i is not a surface particle, then for each particle j in the support domain of i and located on the free surface, a particle j' is created by mirroring i according to j.

Another method to calculate the normal vector is to use the cover vectors [16]. In fact, the direction of the cover vector can be used as an estimation of the direction of the normal vector of the surface.

In SPH, every field variable is evaluated by a smoothing function, thus it seems preferable to apply the surface tension force over a few smoothing lengths (transition band) and not only on one layer of surface particles. Regardless of the interface tracking techniques presented in the previous section, this transition band can be defined by the normal vectors. In fact, the direction and magnitude of the normal vector are only accurate near the interface. In the bulk, the normal vectors have small magnitude with erroneous directions. This may cause a problem when calculating the curvature because in this case, the normalized normal vectors are used. To address this issue, only well defined normal vectors are used in the surface tension calculation by applying the following filtering

$$\vec{n}_i = \begin{cases} \vec{n}_i & , \quad \text{if } |\vec{n}_i| > \varepsilon \\ 0 & , \quad \text{if } |\vec{n}_i| \leq \varepsilon \end{cases} \quad (13)$$

where the value of ε is typically $0.01/dx$ and dx is the initial particle spacing.

With this condition, a transition band consisting of more than one layer of particles is automatically detected near the interface. Thus, the surface tension force is only applied on these particles. However, as explained earlier, with this technique voids and cavities inside the fluid will generate particles inside the transition band which lead to a nonphysical surface tension force. In this case, it seems important to detect surface particles using an appropriate technique. The transition band will consist of the particles that are in the support domain of the surface particles and have a well defined normal vector.

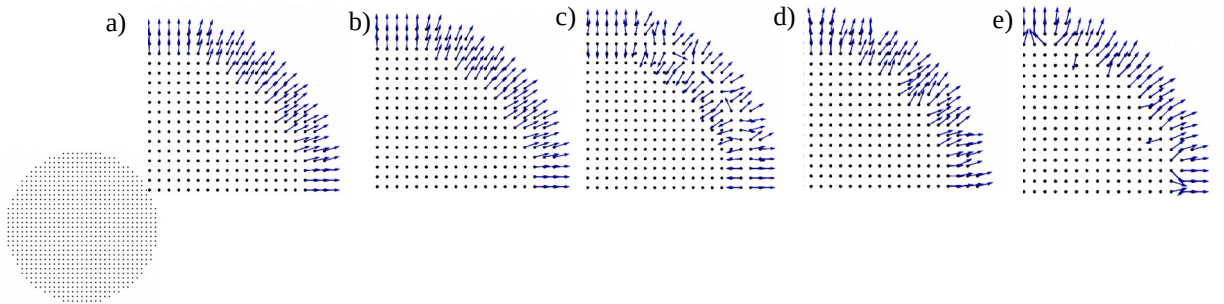


Figure 3: Normal vectors: a) NV- Color gradient, b) NV- Color gradient corrected, c) NV- Russel *et al.*, d) NV- Ordoubadi *et al.* and e) NV- Cover vector

Figure 3 presents a comparison between the different methods presented above. For this comparison, a disk of radius equal to 5 mm is considered. The particle spacing is equal to 0.3 mm and a total

number of 865 particles is considered. The normal vector calculated from the method presented by Russel (c) or from the cover vector (e) are only valid for the first layer of particles.

III.3. Curvature

The curvature at each particle i is calculated as follows

$$k_i = \nabla \cdot \hat{n}_i \quad (14)$$

$$\text{with } \hat{n}_i = \frac{\vec{n}_i}{|\vec{n}_i|} \quad (15)$$

Only the reliable normal vectors should be taken into consideration for the calculation of the curvature. This means that the wrong direction for the normal vectors create a problem also in calculating the curvature. Moreover, the calculation of the curvature is sensitive because it is based on two consecutive derivations of the kernel function.

Here, we are going to compare different methods found in the literature to calculate the curvature (Figure 4). For this comparison, the same disk of radius equal to 5 mm was considered with 865 particles. For the first test, and in order to eliminate the effect of the normal vector directions, prescribed normal vectors are used. We impose the normal vector of particle i to be exactly

$$\vec{n}_i = \vec{r}_i - (\vec{r})_{center} \quad (16)$$

Morris [7] added a normalization factor for the curvature calculation, thus the curvature is obtained by

$$k_i = \frac{\sum_j V_j (\hat{n}_j - \hat{n}_i) \cdot \nabla W_{ij}}{\sum_j V_j W_{ij}} \quad (17)$$

According to Sirotkin et al. [8], with the correction matrix used for calculating the gradient of the kernel function the normalization factor is not required anymore, and the curvature is then calculated as follows

$$k_i = \sum_j V_j (\hat{n}_j - \hat{n}_i) \cdot \nabla \widetilde{W}_{ij} \quad (18)$$

Adami et al. [8] proposed another divergence approximation for calculating the curvature with lacking full support by

$$k_i = d \frac{\sum_j V_j (\hat{n}_j - \hat{n}_i) \cdot \nabla W_{ij}}{\sum_i V_j |r_{ij}| \frac{dW_{ij}}{dr}} \quad (19)$$

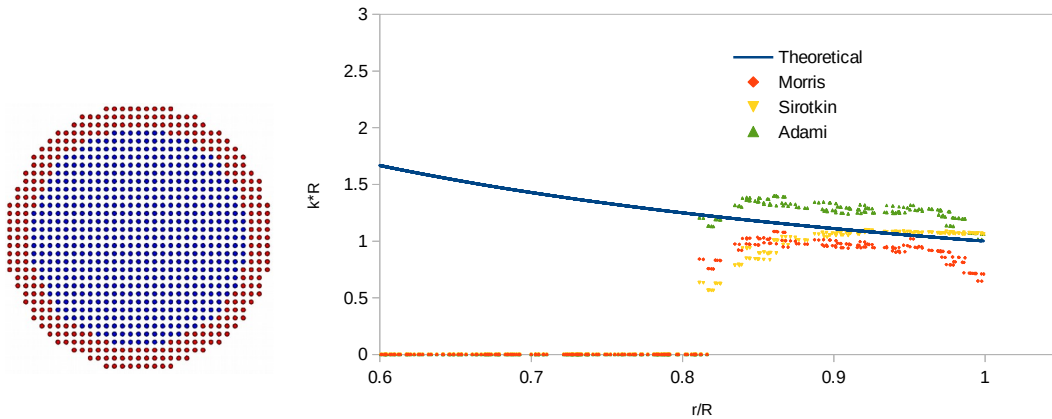


Figure 4: Different methods for curvature estimation

According to the results presented in Figure 4, it seems that the three methods give acceptable results for the curvature estimation. We are more interested in the region close to the free surface ($r/R > 0.95$) where the surface delta function is maximum. In Adami and Morris models, the curvature tends to decrease slightly near the free surface because of the lack of the full support. On the other hand, the correction matrix used by Sirotkin compensates the missing particles near the free surface and hence it gives more accurate results. Note that Ordoubadi *et al.* [10] used the imaginary particles to calculate the curvature based on Eq. (17).

IV. Application of surface tension force

When calculating the surface tension force, we should only consider the surface particles and smooth this force by using an appropriate surface delta function or a kernel function. For example, Ehigiamusoe *et al.* [11] set the surface delta function equal to $1/dx$ at the interface. For the other methods, the smoothing of the force can be done using the norm of the normal vector, subsequently the delta function can be approximated as

$$\delta_s = \lambda |n| \quad (20)$$

where λ is a constant calibration parameter.

The surface tension force should be maximum at the surface or at the tip of sharp corners and it must decrease in magnitude gradually while moving away from the free surface to the interior. The comparison between different surface delta functions is presented in Figure 5. In order to compare them, the normal vectors are normalized to the maximum value depending on each method. The smoothing over the transition band with and without correction are completely different, knowing that the direction of the normal vectors are almost the same.

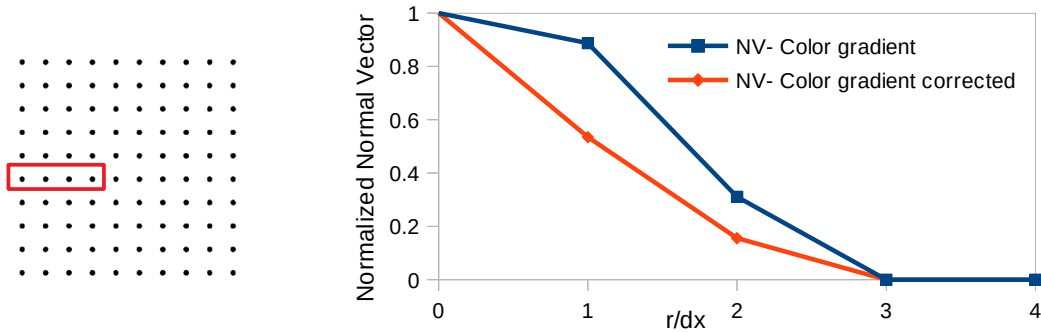


Figure 5: Comparison between the different surface delta functions

In order to obtain a proper surface tension force, many combinations of the different methods presented above for surface characterization were tested. For the surface particle detection, the kernel summation gives good results and it can be combined with the cover vector method for complex geometries. For the normal vector, all the presented methods give acceptable directions, at least for the first layer of surface particle. The crucial differences lay in the definition of the transition band for the curvature calculation and the choice of the smoothing surface delta function. For the curvature calculation, the three methods give good results. If the correction matrix is already calculated, Eq. (18) will be used to calculate the curvature because it is the most accurate. Otherwise, Eq. (17) could be used to minimize the computational cost.

The calculation of the surface properties and the accurate representation of the surface tension plays an important role in the stability of the simulation. However, other parameters should be considered, notably the density evaluation method and the momentum equation discretization. Many combinations can be tested, but we decided to work with the formulation proposed by Adami *et al.* [8] for the momentum equation and the density integration technique for the density evaluation.

To sum up, Table 1 presents the most promising methods/combinations that we decided to explore further in our ongoing study.

ID	Normal vector		Surface delta function + Smoothing		
	Sirotkin <i>et al.</i>	Cover vector	Sirotkin <i>et al.</i>	Morris	Kernel
A	X		X		
B	X		<i>no smoothing</i>		
C		X	<i>no smoothing</i>		

Table 1: Methods/Combinations for surface tension force in SPH

In the next section we present both static and dynamic numerical test cases to validate the models.

V. Numerical examples

V.1. Square droplet

One common test case is the transformation of a square droplet into a circular droplet under the effect of surface tension. For this example, an initial square of $L=1=5$ mm is placed in the center of a square domain ($10*L$). The particle spacing is equal to 0.1 mm and a total number of 2500 particles is considered. The physical properties of water were considered except that a higher viscosity (10 times the viscosity of water) was needed for a stable simulation. For all the test cases a smoothing length of $h=3dx$ is used. Figure 6 presents the initial and final stable shape after $t=0.2$ s of the droplet. By comparing the final results, we can deduce that method C does not give a stable circular droplet even after $t>0.2$ s.

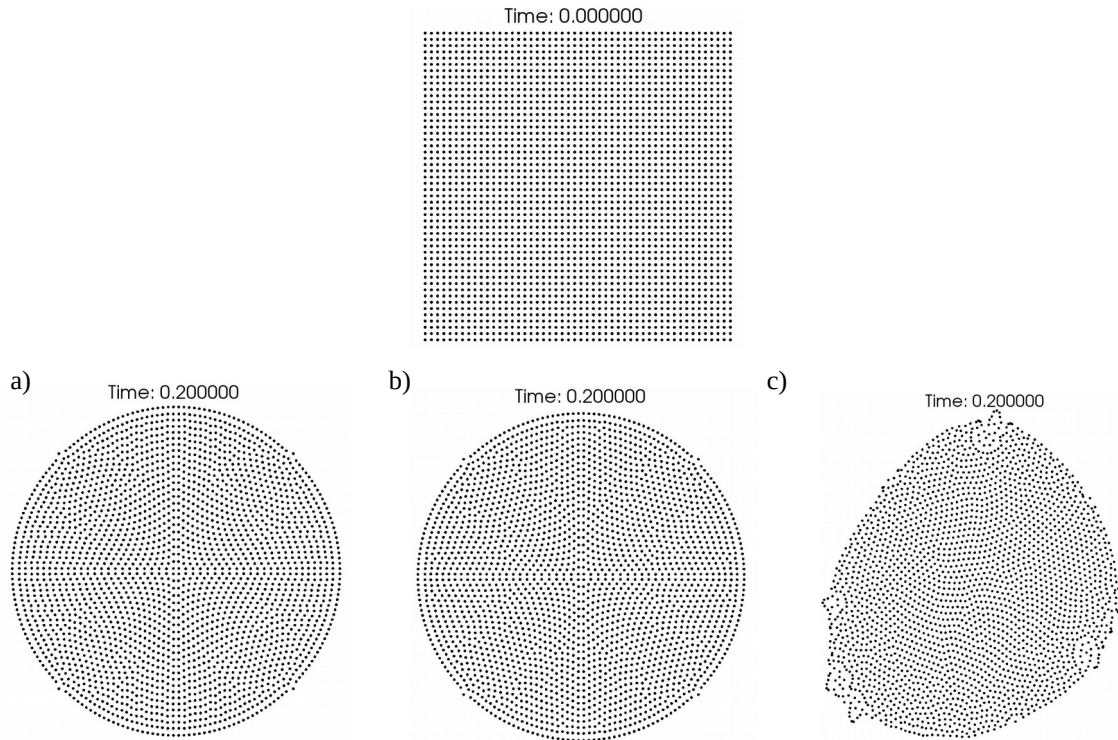


Figure 6: Particle positions at $t=0$ and $t=0.2$ s : a) Method A, b) Method B, and c) Method C

The pressure profile inside the droplet at $t=0.2$ s is compared to the Laplace pressure drop given by Eq. (21) (Figure 7). The pressure profile is almost constant inside the droplet and is equal to the theoretical pressure with some fluctuations near the free surface. The calibration coefficient λ is found equal to 3 for method A. An overall coefficient of around 6.5 is used for method B to compensate in part the drop in the curvature estimated values due to the use of only surface particles.

In methods A and B, this coefficient is independent on the physical size or the initial spacing of the particles.

$$P = \frac{\sigma}{R} = \frac{\sigma \sqrt{\pi}}{L} \quad (21)$$

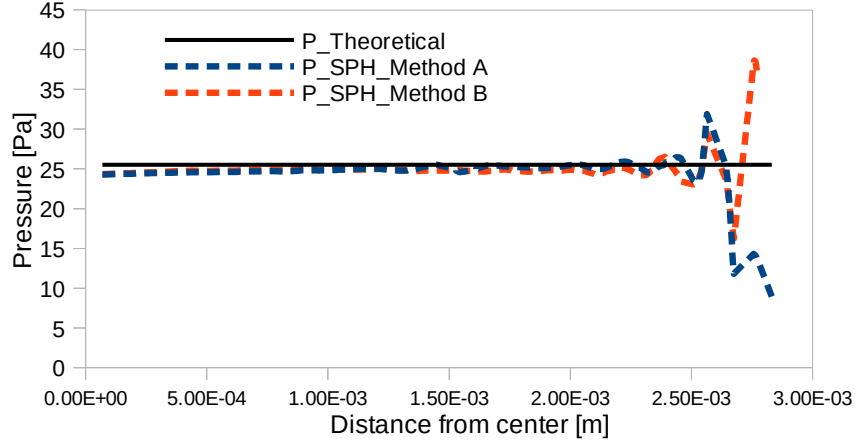


Figure 7: Pressure profile of the droplet at $t=0.2$ s

V.2. Droplet oscillation

An other dynamic test case is the droplet oscillation under the effect of surface tension. Instead of starting from an elliptic droplet, an initial velocity field was prescribed as follows:

$$u_x = u_0 \frac{x}{r_0} \left(1 - \frac{y^2}{r_0 r}\right) * \exp\left(\frac{-r}{r_0}\right) \quad (22)$$

$$u_y = -u_0 \frac{y}{r_0} \left(1 - \frac{x^2}{r_0 r}\right) * \exp\left(\frac{-r}{r_0}\right) \quad (23)$$

The circular droplet of radius equal to 1.7 mm is placed at the center of the computational square domain. The total number of particles is equal to 912 with a particle spacing equal to 0.1 mm. Physical properties of water were considered. However, a dynamic viscosity of $0.003 \text{ Kg.m}^{-1}.\text{s}^{-1}$ is considered. In this example u_0 and r_0 were taken equal to 2 m/s and 0.05 m, respectively. Figure 8 shows the position of the particles at different times for the three methods listed in Table 1. It can be deduced that the three methods give relatively stable results. However, by comparing the particles distribution, we can conclude that the first two methods based on the correction matrix are more accurate.

The distance between the top particle along the y axis and the center of the droplet is plotted over time in Figure 9. According to method A, the SPH period of oscillation is $T_{\text{SPH}}=21.6$ ms. We found good agreement by comparing the SPH period with the theoretical period of oscillations given by:

$$T_{\text{theo}} = 2\pi \sqrt{\frac{R^3 \rho}{s(s^2-1)\sigma}} = 21.2 \text{ ms} \quad , \quad (24)$$

where R is the droplet radius and $s=2$ if the shape of the drop remains close to an ellipse.

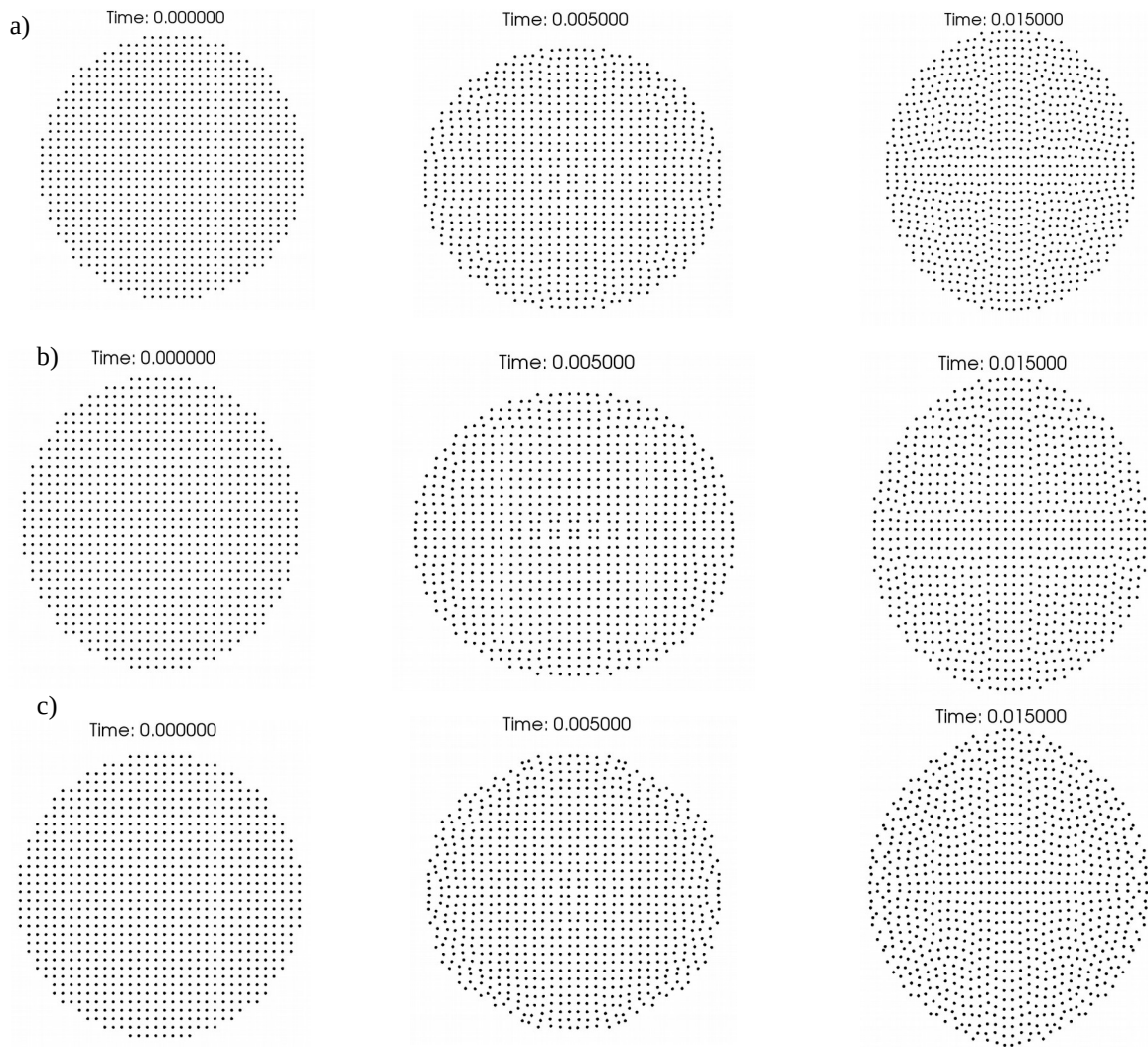


Figure 8: Evolution of the particles position at different time intervals: a) Method A, b) Method B and c) Method C

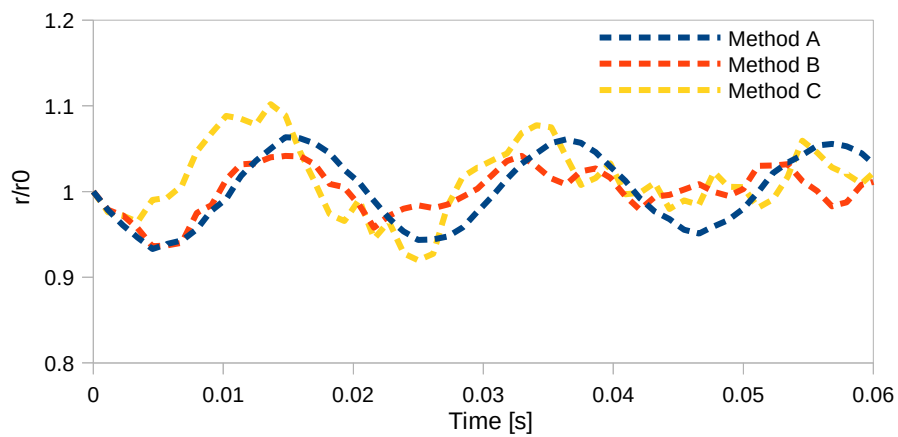


Figure 9: Evolution of the droplet size along the y axis

VI. Conclusions

In this work, we compare methods found in the literature for detecting surface particles, calculating normal vectors and curvature in order to estimate the proper surface tension force for free surface simulations. Other interesting methods can be explored in the future, like for example the reconstruction of the interface to calculate the normal vector and curvature [18].

Basically, once the normal vectors and curvature are correctly obtained the surface tension forces should be easily calculated. However, the choice of the transition band and the surface delta function plays an important role in defining the surface tension force. By comparing the three tested methods, we can conclude that the classical method presented by Sirotkin *et al.* [9] is the most stable one. The use of a transition band in method A is necessary for complex geometries. It ensures that a new surface particle will consider a surface tension force even though the particle is not detected as a surface particle but has at least one surface particle in its neighborhood. Another advantage of this method is the accuracy in calculating the curvature of the free surface.

Moreover, the stability of the simulation depends on many other factors like the pressure force, the viscosity force and the density calculation. These elements have a huge impact on the stability of the simulation. More importantly, the calculation of the density for free surface simulation needs to be adjusted near the free surface.

The objective of our future work is to improve the existing models to simulate low viscosity fluids such as water.

References

- [1] L. B. Lucy, "A numerical approach to the testing of the fission hypothesis," *Astron. J.*, vol. 82, p. 1013, Dec. 1977.
- [2] R. A. Gingold and J. J. Monaghan, "Smoothed particle hydrodynamics: theory and application to non-spherical stars," *Mon. Not. R. Astron. Soc.*, vol. 181, no. 3, pp. 375–389, Dec. 1977.
- [3] A. Tartakovsky and P. Meakin, "Modeling of surface tension and contact angles with smoothed particle hydrodynamics," *Phys. Rev. E*, vol. 72, no. 2, Aug. 2005.
- [4] N. Akinci, G. Akinci, and M. Teschner, "Versatile surface tension and adhesion for SPH fluids," *ACM Trans. Graph.*, vol. 32, no. 6, pp. 1–8, Nov. 2013.
- [5] X. Y. Hu and N. A. Adams, "A multi-phase SPH method for macroscopic and mesoscopic flows," *J. Comput. Phys.*, vol. 213, no. 2, pp. 844–861, Apr. 2006.
- [6] J. . Brackbill, D. . Kothe, and C. Zemach, "A continuum method for modeling surface tension," *J. Comput. Phys.*, vol. 100, no. 2, pp. 335–354, Jun. 1992.
- [7] J. P. Morris, "Simulating surface tension with smoothed particle hydrodynamics," *Int. J. Numer. Methods Fluids*, vol. 33, no. 3, pp. 333–353, Jun. 2000.
- [8] S. Adami, X. Y. Hu, and N. A. Adams, "A new surface-tension formulation for multi-phase SPH using a reproducing divergence approximation," *J. Comput. Phys.*, vol. 229, no. 13, pp. 5011–5021, Jul. 2010.
- [9] F. V. Sirotkin and J. J. Yoh, "A new particle method for simulating breakup of liquid jets," *J. Comput. Phys.*, vol. 231, no. 4, pp. 1650–1674, Feb. 2012.
- [10] M. Ordoubadi, M. Yaghoubi, and F. Yeganehdoust, "Surface tension simulation of free surface flows using smoothed particle hydrodynamics," *Sci. Iran.*, vol. 24, no. 4, pp. 2019–2033, Aug. 2017.
- [11] N. N. Ehigiamusoe, S. Maxutov, and Y. C. Lee, "Modeling surface tension of a two-dimensional droplet using smoothed particle hydrodynamics: Modeling surface tension of a two-dimensional droplet using SPH," *Int. J. Numer. Methods Fluids*, vol. 88, no. 7, pp. 334–346, Nov. 2018.
- [12] M. A. Russell, A. Souto-Iglesias, and T. I. Zohdi, "Numerical simulation of Laser Fusion Additive Manufacturing processes using the SPH method," *Comput. Methods Appl. Mech. Eng.*, vol. 341, pp. 163–187, Nov. 2018.
- [13] J. Bonet and T.-S. L. Lok, "Variational and momentum preservation aspects of Smooth Particle Hydrodynamic formulations," *Comput. Methods Appl. Mech. Eng.*, vol. 180, no. 1–2, pp. 97–115, Nov. 1999.
- [14] J. J. Monaghan, "Smoothed Particle Hydrodynamics," *Annu. Rev. Astron. Astrophys.*, vol. 30, no. 1, pp. 543–574, Sep. 1992.

- [15] J. J. Monaghan, “Smoothed particle hydrodynamics,” *Rep. Prog. Phys.*, vol. 68, no. 8, pp. 1703–1759, Aug. 2005.
- [16] A. Barescaso, H. Terissa, and C. F. Naa, “Simple free-surface detection in two and three-dimensional SPH solver,” *ArXiv13094290 Phys.*, Sep. 2013.
- [17] G. A. Dilts, “Moving least-squares particle hydrodynamics II: conservation and boundaries,” *Int. J. Numer. Methods Eng.*, vol. 48, no. 10, pp. 1503–1524, Aug. 2000.
- [18] M. Zhang, “Simulation of surface tension in 2D and 3D with smoothed particle hydrodynamics method,” *J. Comput. Phys.*, vol. 229, no. 19, pp. 7238–7259, Sep. 2010.